

3-2015

# Temperature dependent c-axis hole mobilities in rubrene single crystals determined by time-of-flight

Russell L. Lidberg

*St. Cloud State University*, [rlidberg@stcloudstate.edu](mailto:rlidberg@stcloudstate.edu)

Tom J. Pundsack

*University of Minnesota - Twin Cities*

Neale O. Haugen

*University of Toledo*


Lucas R. Johnstone

*Georgia Institute of Technology - Main Campus*

C. Daniel Frisbie

*University of Minnesota - Twin Cities*

Follow this and additional works at: [https://repository.stcloudstate.edu/phys\\_facpubs](https://repository.stcloudstate.edu/phys_facpubs)

 Part of the [Biological and Chemical Physics Commons](#), [Condensed Matter Physics Commons](#), [Materials Chemistry Commons](#), [Materials Science and Engineering Commons](#), and the [Physical Chemistry Commons](#)

---

## Recommended Citation

Lidberg, Russell L.; Pundsack, Tom J.; Haugen, Neale O.; Johnstone, Lucas R.; and Frisbie, C. Daniel, "Temperature dependent c-axis hole mobilities in rubrene single crystals determined by time-of-flight" (2015). *Physics and Astronomy Faculty Publications*. 6.  
[https://repository.stcloudstate.edu/phys\\_facpubs/6](https://repository.stcloudstate.edu/phys_facpubs/6)

This Article is brought to you for free and open access by the Department of Physics and Astronomy at theRepository at St. Cloud State. It has been accepted for inclusion in Physics and Astronomy Faculty Publications by an authorized administrator of theRepository at St. Cloud State. For more information, please contact [rswexelbaum@stcloudstate.edu](mailto:rswexelbaum@stcloudstate.edu).

# Temperature dependent c-axis hole mobilities in rubrene single crystals determined by time-of-flight

Tom J. Pundsack,<sup>1,a)</sup> Neale O. Haugen,<sup>1,b)</sup> Lucas R. Johnstone,<sup>1,c)</sup> C. Daniel Frisbie,<sup>2</sup> and Russell L. Lidberg<sup>1,d)</sup>

<sup>1</sup>Department of Physics and Astronomy, St. Cloud State University, St. Cloud, Minnesota 56301, USA

<sup>2</sup>Department of Chemical Engineering and Materials Science, University of Minnesota, Minneapolis, Minnesota 55455, USA

(Received 9 January 2015; accepted 28 February 2015; published online 17 March 2015)

Hole mobilities ( $\mu$ ) in rubrene single crystals (space group Cmca) along the crystallographic **c**-axis have been investigated as a function of temperature and applied electric field by the time-of-flight method. Measurements demonstrate an inverse power law dependence on temperature, namely,  $\mu = \mu_0 T^{-n}$  with  $n = 1.8$ , from room temperature down to 180 K. At 296 K, the average value of  $\mu$  was found to be  $0.29 \text{ cm}^2/\text{Vs}$  increasing to an average value of  $0.70 \text{ cm}^2/\text{Vs}$  at 180 K. Below 180 K a decrease in mobility is observed with further cooling. Overall, these results confirm the anisotropic nature of transport in rubrene crystals as well as the generality of the inverse power law temperature dependence that is observed for field effect mobility measurements in the **a-b** crystal plane. © 2015 AIP Publishing LLC. [<http://dx.doi.org/10.1063/1.4914975>]

Interest in the use of conjugated organic materials as the active element in electrical and electro-optical devices is driven by their processing and mechanical advantages and by the ability to chemically tune their electronic and optical properties. Organic semiconductors have been studied for applications in light-emitting diodes, photovoltaics, field effect transistors, chemical sensors, and flexible displays.<sup>1–11</sup> The design and implementation of these materials requires a fundamental understanding of their physical properties. The transport of charge carriers (electrons or holes), in particular, is a key component of device performance. The relationship between the molecular structure of organic semiconducting materials in the solid state and charge carrier transport remains a critical issue in the design of organic based electronic devices.

In order to improve understanding of the charge transport mechanisms, it is desirable to work with high purity, highly ordered crystal systems.<sup>12,13</sup> The use of conjugated small molecular species such as the oligoacenes (anthracene, pentacene, tetracene, and rubrene) has provided the experimentalist an avenue to grow crystals that are of high purity and that possess a high degree of structural order.<sup>14–18</sup>

Two commonly used techniques for determining charge carrier mobilities in oligoacenes are field-effect transistor (FET) measurements<sup>17,19,20</sup> and time-of-flight (TOF) measurements.<sup>19,21,22</sup> FET measurements probe transport in the **a-b** plane at or near the surface of the crystal. TOF measurements are routinely used for measuring mobilities through the bulk of the material, typically corresponding to the **c**-lattice parameter of oligoacenes.

Of the oligoacenes studied to date, rubrene (5,6,11,12-tetraphenyltetracene) single crystals have shown the highest measured field effect hole mobilities of  $20 \text{ cm}^2/\text{Vs}$  at 300 K in the **b**-axis direction.<sup>23</sup> These field effect results have also confirmed the anisotropic nature of transport for the **a-b** surface plane with measured hole mobilities along the **b**-axis three times larger than along the **a**-axis. Time-of-flight measurements along the **c**-axis direction of rubrene single crystals have been reported by Williams.<sup>24</sup> His results showed hole mobilities of  $0.5 \text{ cm}^2/\text{Vs}$  at room temperature with mobilities increasing to  $2 \text{ cm}^2/\text{Vs}$  at 473 K.

In this paper, we report TOF hole drift mobility measurements in single crystals of rubrene in the **c**-axis direction as a function of temperature (140–300 K) and electric field (43–79 kV/cm). Five different crystals were examined. Mobility measurements were conducted at room temperature under atmospheric conditions and at low temperature in a He cryostat at a vacuum of 50 mTorr.

Single crystals of rubrene were grown by physical vapor transport in a flowing high purity argon atmosphere.<sup>25</sup> Rubrene grown by physical vapor transport (Fig. 1) forms

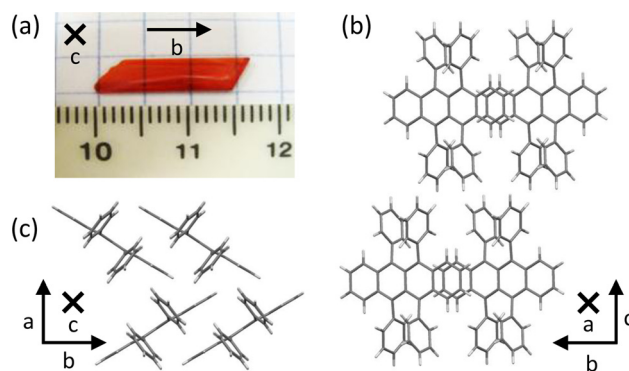


FIG. 1. (a) Typical plate-like rubrene crystal grown by physical vapor transport. (b) Rubrene crystal structure in the **b-c** plane. (c) Rubrene crystal structure in the **a-b** plane. Crystal axes (**a**, **b**, and **c** directions) depicted by arrows.

<sup>a)</sup>Present Address: Department of Chemistry, University of Minnesota, Minneapolis, Minnesota 55455, USA.

<sup>b)</sup>Present Address: Department of Physics and Astronomy, The University of Toledo, Toledo, Ohio 43606, USA.

<sup>c)</sup>Present Address: Department of Chemistry and Biochemistry, Georgia Institute of Technology, Atlanta, Georgia 30332, USA.

<sup>d)</sup>rlidberg@stcloudstate.edu

orthorhombic crystals with slipped  $\pi$ -stack packing and lattice constants of  $a = 7.18 \text{ \AA}$ ,  $b = 14.43 \text{ \AA}$ , and  $c = 26.90 \text{ \AA}$ . The crystals grow as flat platelets with the large facet corresponding to the **a-b** surface plane and the **c**-axis perpendicular to the surface. Rubrene, 99% sublimed grade, was purchased from Aldrich and used as received. A sublimation temperature of  $285 \text{ }^\circ\text{C}$  was used and a temperature gradient of approximately  $3 \text{ }^\circ\text{C/cm}$  maintained throughout the growth tube. Both crystals of plate and needle motifs were obtained during the growth process. Plate-like crystals were selected for use in the TOF experiments. Plate crystals with dimensions in the range of  $1 \text{ cm} \times 0.5 \text{ cm} \times 100 \text{ }\mu\text{m}$  (length  $\times$  width  $\times$  thickness) were routinely grown as seen in Fig. 1. Crystal thicknesses, in the **c**-direction, typically ranged from 60 to  $150 \text{ }\mu\text{m}$ . Crystals were inspected under cross polarizers to assure they were single crystals and no twinning was present in the area of analysis.<sup>26</sup>

In TOF measurements, electron-hole pairs are photo-excited near the surface of the material by a short pulse of radiation, typically a laser pulse, and transported through the sample by an electric field generated by applying a voltage to two electrodes located on the top and bottom faces of the crystal. The transit time,  $t_{tr}$ , of the resulting current pulse is determined and the carrier mobility,  $\mu$ , is calculated using the crystal thickness,  $L$ , and the electric field,  $E$ , induced by the applied voltage,  $V$ :

$$\mu = \frac{L}{E t_{tr}} = \frac{L^2}{V t_{tr}}. \quad (1)$$

The shape of the resulting current pulse can reveal the presence and degree of structural defects and traps in the bulk of the crystal. In an ideal crystal with no trapping, the current pulse has a distinct plateau and a sharp decay point indicating the transit time. In systems with more disorder or deep traps, current pulses can have less distinct decay points with a trailing edge that decays to the baseline.

Selected crystals were prepared for TOF analysis by sputtering silver contacts on the top and bottom faces of the crystals directly opposite each other using a Denton Desk IV sputter coater. Contacts were  $3 \text{ mm} \times 3 \text{ mm} \times 10 \text{ nm}$  thick. The crystals were then mounted on a home-made stage in a RMC-Cryosystems closed cycle He cryostat. Leads were connected to the crystal using silver paste. DC voltage was applied to the crystal using a Keithly 2410 Sourcemeter. A PTI GL-3300 nitrogen laser ( $337 \text{ nm}$ , pulse width of  $800 \text{ ps}$ ) with random polarization, was used to create charge carriers in the sample. The crystals were excited at normal incidence to the **a-b** crystal facet. The intensity of the laser pulse was adjusted using neutral density filters to ensure no internal space charge effects were encountered due to excessive carrier density.<sup>21</sup> Rubrene crystals have a high optical absorbance with an absorption coefficient greater than  $1 \times 10^4 \text{ cm}^{-1}$  at  $337 \text{ nm}$ ,<sup>27</sup> resulting in an absorption length of less than  $1 \text{ }\mu\text{m}$ . The TOF photocurrent transient was measured as a voltage drop across a  $1 \text{ k}\Omega$  resistor using a Tektronix DPO7104  $1 \text{ GHz}$  oscilloscope. Crystals were examined as a function of applied voltage at constant temperature ( $296 \text{ K}$ ) and as a function of temperature ( $140\text{--}296 \text{ K}$ ) at constant voltage.

A typical TOF hole pulse for rubrene at room temperature is shown in Fig. 2(a). The transit time,  $t_{tr}$ , which is the time for the carrier pulse to cross the crystal, is marked. A clearer indication of  $t_{tr}$  is obtained by a  $\log V$  versus  $\log t$  plot. The knee of the curve formed by asymptotes drawn from the plateau and tail of the plot is taken as the transit time (Fig. 2(b)).

Room temperature data were collected from five different crystals and are shown in Table I. Two of the room temperature data points (crystals 1 and 2) were collected at atmospheric pressure in air. The mobility for crystal 2 was calculated from the results of varying the applied voltage, as discussed below. The other three room temperature data points (crystals 3, 4, and 5) were collected while the crystals were mounted in a He cryostat and were measured at a pressure of  $50 \text{ mTorr}$ . The average mobility of the five room temperature measurements was  $0.29 \pm 0.05 \text{ cm}^2/\text{Vs}$ . This is comparable to the room temperature hole mobility value of approximately  $0.5 \text{ cm}^2/\text{Vs}$  reported by Williams.<sup>24</sup>

Fig. 3 shows the linear relation between the measured inverse transit times and electric field for crystal 2. By using the slope of this plot along with the thickness of the crystal,  $L$ , the mobility was calculated to be  $0.24 \text{ cm}^2/\text{Vs}$  in agreement with room temperature mobilities of the other crystals in this study.

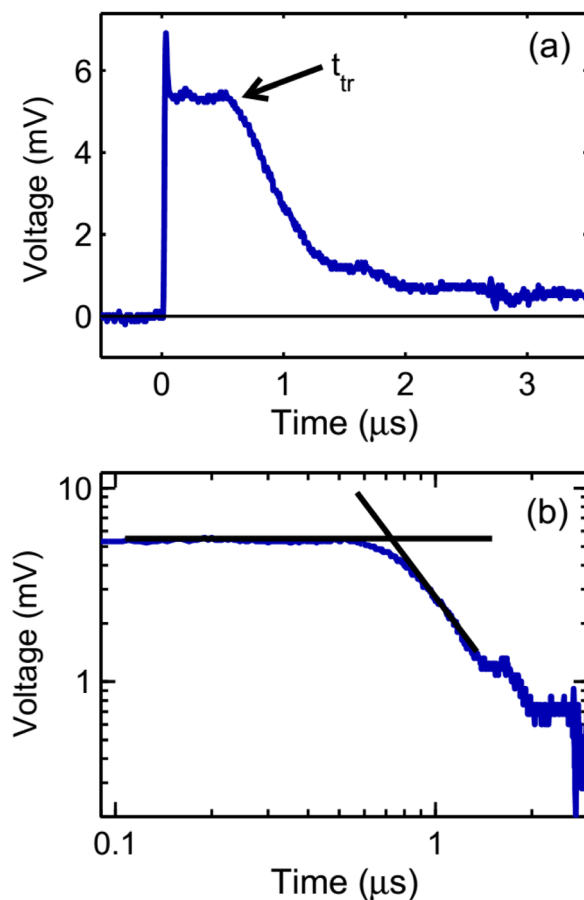


FIG. 2. (a) TOF hole signal obtained from crystal 1.  $T = 296 \text{ K}$ ,  $L = 145 \text{ }\mu\text{m}$ ,  $V = 800 \text{ V}$ ,  $E = 55 \text{ kV/cm}$ ,  $t_{tr} = 0.71 \text{ }\mu\text{s}$ ,  $\mu = 0.37 \text{ cm}^2/\text{Vs}$ . Transit time noted as  $t_{tr}$ . (b)  $\log V$  versus  $\log t$  plot of Fig. 2(a). Intercept of asymptotes represents  $t_{tr}$ .

TABLE I. Rubrene room temperature TOF mobilities (296 K) from five different rubrene crystals under different conditions.

Crystal	Source	Mobility (cm <sup>2</sup> /Vs)
1	Atmospheric (Fig. 2)	0.37
2	Voltage bias data (Fig. 3)	0.24
3	Cryostat (50 mTorr)	0.27
4	Cryostat (50 mTorr)	0.27
5	Cryostat (50 mTorr)	0.31

Charge carrier mobilities are also influenced by temperature. Below room temperature, these single crystals generally exhibit an inverse power law dependence,  $\mu = \mu_0 T^{-n}$  (where  $n = 1-3$ ). That is,  $\mu$  increases with decreasing temperature. This behavior can change at a critical lower temperature typically near 170–180 K (for rubrene), where transport becomes activated.<sup>23,28,29</sup> This change as temperature decreases can be attributed to trap states that have trapping energies larger than  $k_B T$  or to structural phase transitions in the crystal at a given temperature.<sup>23,30,31</sup> Above room temperature, crystal carrier transport is also thermally activated (Arrhenius-like).<sup>32</sup>

Temperature dependent measurements were performed on three separate crystals. Two crystals (crystals 3 and 4) were measured from 296 to 140 K. A third crystal (crystal 5) was measured from 296 to 180 K. No signal was obtained from crystal 5 below 180 K. Upon removing crystal 5 from the cryostat it was noted that the crystal had cracked. The log V versus log t plots of the TOF signals from crystal 5 are shown in Fig. 4 for temperatures of 296, 240, and 180 K. Transit times, taken as the knee of the plots, decreased with decreasing temperature corresponding to an increase in hole mobility.

The  $\mu$ -temperature behavior for crystals 3–5 are summarized in Fig. 5(a). These data show an increase in mobility with a decrease in temperature from 296 K to 180 K. The average hole mobility at 180 K for crystals 3, 4, and 5 was  $0.70 \pm 0.12$  cm<sup>2</sup>/Vs with crystal 5 reaching a maximum value of  $0.84$  cm<sup>2</sup>/Vs at 180 K. For crystals 3 and 4, the mobilities start to decrease with further decrease in temperature at around 170–180 K. This was also observed in FET

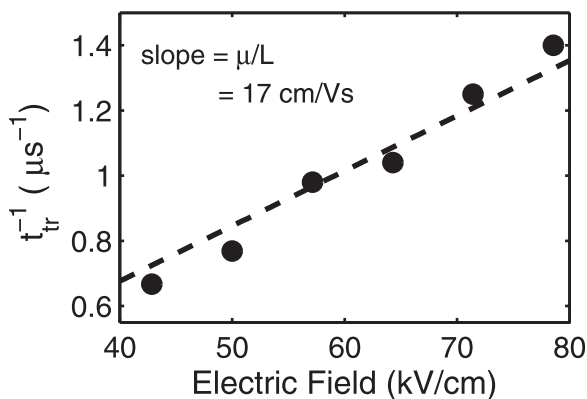


FIG. 3. Voltage dependence of transit time from crystal 2.  $L = 140$   $\mu\text{m}$ ,  $V = 600$ – $1100$  V,  $E = 43$ – $79$  kV/cm. Slope =  $17$  cm/Vs. Calculated hole mobility,  $\mu = 0.24$  cm<sup>2</sup>/Vs.

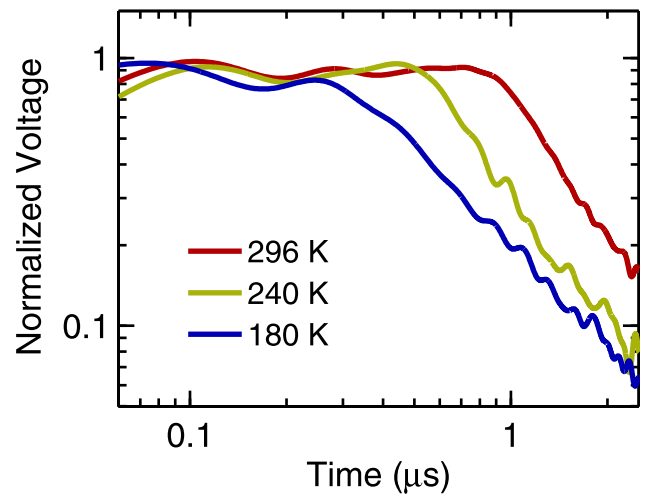


FIG. 4. Temperature dependent log V vs. log t TOF pulses from Crystal 5.  $L = 105$   $\mu\text{m}$ ,  $V = 400$  V,  $E = 38$  kV/cm. Transit times: 296 K,  $t_{tr} = 0.88$   $\mu\text{s}$ ; 240 K,  $t_{tr} = 0.53$   $\mu\text{s}$ ; 180 K,  $t_{tr} = 0.33$   $\mu\text{s}$ .

mobility measurements and occurred in approximately the same temperature range.<sup>23</sup>

The low temperature hole mobilities in the c-axis for crystals 3, 4, and 5 showed an inverse power law temperature dependence in the range from 296–180 K with  $n = 1.8 \pm 0.2$ , as shown in Fig. 5(b). These results support earlier low

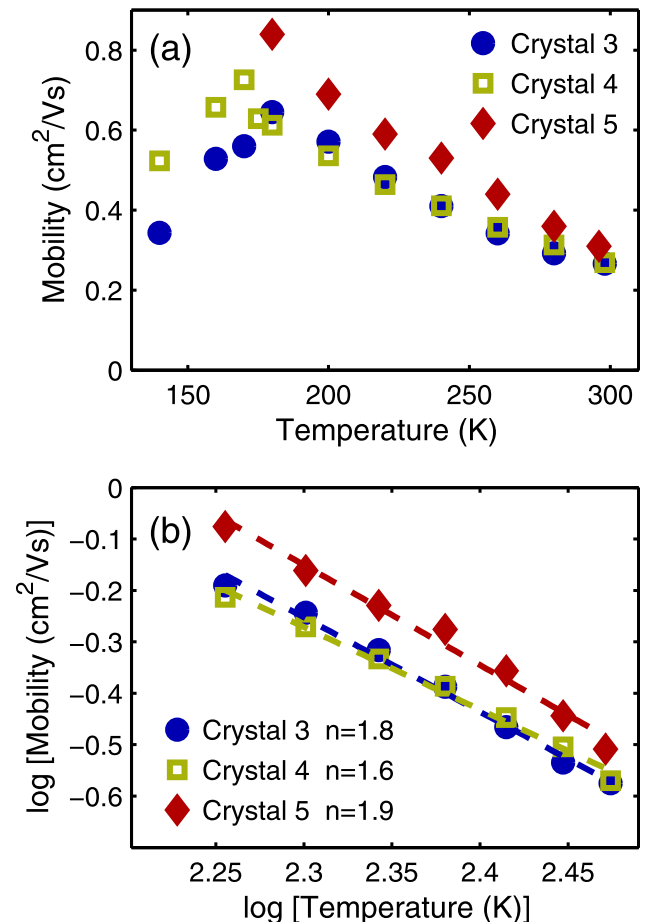


FIG. 5. (a) Temperature dependence of bulk TOF hole mobilities for crystals 3, 4, and 5.  $V = 400$  V. (b) Log-log plot of the mobility data in the band transport region ( $T = 180$ – $296$  K). Dashed lines show linear fits to the log-log data:  $\log(\mu) = \log(\mu_0) - n \log(T)$ .

temperature FET measurements on rubrene crystals in the **a-b** crystal directions that also showed increased mobilities from room temperature to 180 K.<sup>23</sup> The  $n$  value is in line with a value of  $n = 2$  determined from mobilities measured over the same temperature range in the conduction channel of a rubrene single crystal based FET using Hall effect measurements.<sup>17</sup> Additionally, these  $n$  values are in close agreement with computational results obtained by Troisi for a rubrene crystal over the same temperature range, where a value of  $n = 2.1$  was reported.<sup>33</sup>

It should be noted that the power law dependence of mobility on temperature in the **c**-axis direction is a bit surprising. In FET measurements of transport in the **a-b** plane, the power law dependence is taken to be a sign of “band-like” transport. Band-like behavior is thought to arise from the strong intermolecular overlap integrals in the **a-b** plane of rubrene. However, quantum chemical calculations indicate that the overlap integrals are weaker in the **c**-axis direction.<sup>34</sup> The weaker electronic coupling might be expected to lead to thermally activated transport along the **c**-axis, and yet this is not what we observe. Further work is needed to understand whether the explanations put forth in the literature for inverse power law behavior in the **a-b** plane are also applicable to **c**-axis transport. Interestingly, we note that Karl and colleagues also previously reported inverse power law dependence for TOF mobilities along the **c**-axis of anthracene.<sup>14</sup>

In summary, the hole mobility was measured along the **c**-axis crystallographic direction of rubrene single crystals. Low temperature results showed power law temperature dependent transport in the range of 180–296 K. At  $\sim 180$  K, the hole mobility reached a maximum of  $0.84 \text{ cm}^2/\text{Vs}$  (crystal 5) with an average value of  $0.70 \text{ cm}^2/\text{Vs}$  (crystals 3, 4, and 5), increasing from a room temperature value of  $0.29 \text{ cm}^2/\text{Vs}$  (average of 5 crystals). Below 180 K a decrease in mobility was seen (crystals 3 and 4). These measurements support the anisotropic nature of carrier mobility, low temperature power law dependence, and decrease of mobility due to trap states or crystal structure rearrangement at 180 K observed in the **a-b** plane of rubrene crystals measured using FET techniques.

<sup>1</sup>L. Zang, Y. Che, and J. S. Moore, *Acc. Chem. Res.* **41**, 1596 (2008).

<sup>2</sup>J. Anthony, *Angew. Chem. Int. Ed.* **47**, 452 (2008).

- <sup>3</sup>T. Hasegawa and J. Takeya, *Sci. Technol. Adv. Mater.* **10**, 024314 (2009).
- <sup>4</sup>Y. Yamashita, *Sci. Technol. Adv. Mater.* **10**, 024313 (2009).
- <sup>5</sup>H. Dong, C. Wang, and W. Hu, *Chem. Commun.* **46**, 5211 (2010).
- <sup>6</sup>A. Mishra and P. Bäuerle, *Angew. Chem. Int. Ed.* **51**, 2020 (2012).
- <sup>7</sup>K.-J. Baeg, M. Binda, D. Natali, M. Caironi, and Y.-Y. Noh, *Adv. Mater.* **25**, 4267 (2013).
- <sup>8</sup>S. Ahmad, *J. Polym. Eng.* **34**, 279 (2014).
- <sup>9</sup>H.-H. Fang, J. Yang, J. Feng, T. Yamao, S. Hotta, and H.-B. Sun, *Laser Photonics Rev.* **8**, 687 (2014).
- <sup>10</sup>B. Kumar, B. K. Kaushik, and Y. Negi, *J. Mater. Sci. - Mater. Electron.* **25**, 1 (2014).
- <sup>11</sup>H. Siringhaus, *Adv. Mater.* **26**, 1319 (2014).
- <sup>12</sup>C. Reese and Z. Bao, *J. Mater. Chem.* **16**, 329 (2006).
- <sup>13</sup>V. Podzorov, *MRS Bull.* **38**, 15 (2013).
- <sup>14</sup>N. Karl and J. Marktanner, *Mol. Cryst. Liq. Cryst.* **355**, 149 (2001).
- <sup>15</sup>V. Podzorov, S. Sysoev, E. Loginova, V. Pudalov, and M. Gershenson, *Appl. Phys. Lett.* **83**, 3504 (2003).
- <sup>16</sup>R. De Boer, M. Jochemsen, T. Klapwijk, A. Morpurgo, J. Niemax, A. Tripathi, and J. Pflaum, *J. Appl. Phys.* **95**, 1196 (2004).
- <sup>17</sup>M. Gershenson, V. Podzorov, and A. Morpurgo, *Rev. Mod. Phys.* **78**, 973 (2006).
- <sup>18</sup>M. Kotani, K. Kakinuma, M. Yoshimura, K. Ishii, S. Yamazaki, T. Kobori, H. Okuyama, H. Kobayashi, and H. Tada, *Chem. Phys.* **325**, 160 (2006).
- <sup>19</sup>A. Kokil, K. Yang, and J. Kumar, *J. Polym. Sci., Part B: Polym. Phys.* **50**, 1130 (2012).
- <sup>20</sup>C. R. Newman, C. D. Frisbie, D. A. da Silva Filho, J.-L. Brédas, P. C. Ewbank, and K. R. Mann, *Chem. Mater.* **16**, 4436 (2004).
- <sup>21</sup>W. E. Spear, *J. Non-Cryst. Solids* **1**, 197 (1969).
- <sup>22</sup>M. Pope and C. E. Swenberg, *Electronic Processes in Organic Crystals and Polymers*, 2nd ed. (Oxford University Press, 1999), p. 709.
- <sup>23</sup>V. Podzorov, E. Menard, A. Borissov, V. Kiryukhin, J. Rogers, and M. Gershenson, *Phys. Rev. Lett.* **93**, 086602 (2004).
- <sup>24</sup>W. Williams, *Discuss. Faraday Soc.* **51**, 61 (1971).
- <sup>25</sup>R. Laudise, C. Kloc, P. Simpkins, and T. Siegrist, *J. Crys. Growth* **187**, 449 (1998).
- <sup>26</sup>J. Vrijmoeth, R. Stok, R. Veldman, W. Schoonveld, and T. Klapwijk, *J. Appl. Phys.* **83**, 3816 (1998).
- <sup>27</sup>P. Irkhin, A. Ryzanskiy, M. Koehler, and I. Biaggio, *Phys. Rev. B* **86**, 085143 (2012).
- <sup>28</sup>W. C. Germs, K. Guo, R. Janssen, and M. Kemerink, *Phys. Rev. Lett.* **109**, 016601 (2012).
- <sup>29</sup>N. A. Minder, S. Ono, Z. Chen, A. Facchetti, and A. F. Morpurgo, *Adv. Mater.* **24**, 503 (2012).
- <sup>30</sup>U. Sondermann, A. Kutoglu, and H. Bassler, *J. Phys. Chem.* **89**, 1735 (1985).
- <sup>31</sup>O. D. Jurchescu, A. Meetsma, and T. T. Palstra, *Acta Crystallogr., Sect. B* **62**, 330 (2006).
- <sup>32</sup>V. Coropceanu, J. Cornil, D. A. da Silva Filho, Y. Olivier, R. Silbey, and J.-L. Brédas, *Chem. Rev.* **107**, 926 (2007).
- <sup>33</sup>A. Troisi, *Adv. Mater.* **19**, 2000 (2007).
- <sup>34</sup>D. A. da Silva Filho, E.-G. Kim, and J.-L. Brédas, *Adv. Mater.* **17**, 1072 (2005).